ChemPubSoc Europe

DOI: 10.1002/open.201700059

Open Access ChemistryOPEN Full Papers

Synthesis of Wavelength-Shifting Fluorescent DNA and RNA with Two Photostable Cyanine–Styryl Dyes as the Base Surrogate Pair

Jeannine Steinmeyer,[a] Franziska Rönicke,[a] Ute Schepers,[b] and Hans-Achim Wagenknecht*[a]

Two nucleic acid building blocks were synthesized, consisting of two photostable green- and red-emitting cyanine–styryl dyes and (*S*)-3-amino-1,2-propanediol as a substitute for the ribofuranoside, and incorporated as base-pair surrogates by using automated phosphoramidte chemistry in the solid phase. The optical properties and, in particular, the energy-transfer properties were screened in a range of DNA duplexes, in which the "counter bases" of the two dyes were varied and the distance between the two dyes was enlarged to up to three intervening adenosine–thymidine pairs. The DNA duplex with the best optical properties and the best red/green emission ratio as the readout bore adenosine and thymidine opposite to the dyes, and the two dyes directly adjacent to each other as the base surrogate pair. This structural arrangement can be transferred to RNA to obtain similarly fluorescent RNA probes. Representatively, the positively evaluated DNA duplex was applied to verify the fluorescence readout in living HeLa cells by using fluorescence confocal microscopy.

1. Introduction

Molecular imaging is a potent technique to visualize intracellular structures and to observe biomolecules inside cells in real time.[1] Labeling nucleic acids with bright fluorescent probes for molecular imaging is important with respect to both the central functions of DNA and RNA inside cells and the delivery of exogenous nucleic acids into cells and organisms.[2] From an organochemical point of view, the advantage of nucleic acids is that they are synthesized from building blocks by using automated chemistry in the solid phase. Fluorescent labeling can be achieved by providing the corresponding fluorophores directly as DNA building blocks,[3] or through reactive building blocks and post-synthetic labeling.[3b,4] With respect to the cationic character of a significant majority of potent DNA- and RNA-labeling dyes as base surrogates, the 2′-deoxy-ribofuranosides had to be replaced by a linker that lacks the hydrolytically labile glycosidic bond and, hence, provides sufficient chemical stability. We applied (*S*)-3-amino-1,2-propanediol,[3a] whereas other groups used D-threoninol[5] or cyclopentanes[6] for the same purpose. This approach worked for several dyes, including ethidium,[7] BODIPY,[8] thiazole orange and red,[9] and other functional molecules.[3a] In particular, thiazole orange and red were combined in an inter-strand manner to promote an efficient energy transfer between them.[10] This DNA and RNA base-substitution approach allowed us to develop wavelength-shifting fluorescent probes ("DNA and RNA traffic lights") as a powerful tool for molecular imaging,[11] evidenced especially for siRNA constructs.[12] The thiazole-derived dyes, however, show a low photostability that limits their imaging applicability.[13] Recently, we developed a broad range of structurally related cyanine–styryl dyes with blue, green, yellow, and red emission and, more importantly, with significantly improved photostability.[14] Herein, we report on the synthesis of two new DNA/RNA building blocks, **5** and **6,** based on the photostable green- and red-emitting cyanine–styryl dyes **1** and **2**, their incorporation into DNA and RNA double strands ($\mathbf{D^1}$ and $\mathbf{D^2}$), and their energy-transfer properties (Scheme 1) in vitro and in living cells.

[a] *J. Steinmeyer, Dr. F. Rönicke, Prof. Dr. H.-A. Wagenknecht*
Institute of Organic Chemistry
Karlsruhe Institute of Technology (KIT)
Fritz-Haber-Weg 6, 76131 Karlsruhe (Germany)
E-mail: Wagenknecht@kit.edu

[b] *Prof. Dr. U. Schepers*
Institute of Toxicology and Genetics
Karlsruhe Institute of Technology (KIT)
Hermann-von-Helmholtz-Platz 1
76344 Eggenstein-Leopoldshafen (Germany)

Supporting Information and the ORCID identification number(s) for the author(s) of this article can be found under https://doi.org/10.1002/open.201700059.

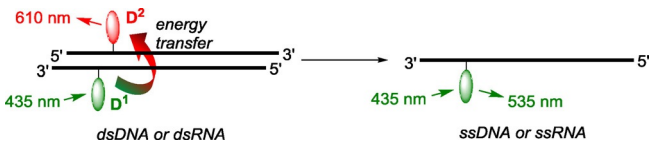

Scheme 1. Principle of wavelength-shifting DNA and RNA "traffic lights": Excitation of the green emitting dye **1** ($\mathbf{D^1}$) in the double strand leads to efficient energy transfer to dye **2** ($\mathbf{D^2}$) and yields red emission, whereas the single strand shows green fluorescence.

2. Results and Discussion

The synthesis of the two nucleic acid building blocks is straightforward, starting from the hydroxypropylated dyes **1**[15] and **2**[16] that were synthesized according to our previously published protocols (Scheme 2). The reaction with carbonyldiimidazole links the dyes to the tritylated (*S*)-3-amino-1,2-propanediole **3** through a carbamate group. Phosphitylation of the remaining secondary hydroxy groups of the intermediate compounds **4** and **5** yield the phosphoramidites **6** and **7**, respectively. Those were solved in dichloromethane (0.1 M) and applied for automated oligonucleotide synthesis. Compared to commercially available building blocks, the coupling time for **6** and **7** was drastically enhanced with intervening washing steps.[17] For RNA synthesis, CPG columns with 2′-acetyl-protecting groups were applied, which require a special cleavage protocol. To avoid degradation of the dyes during DNA/RNA cleavage and workup, the commercially available "ultramild" cleavable building blocks were used.[18] All synthesized oligonucleotides were purified by using semi-preparative HPLC and identified with MALDI-TOF mass spectrometry (see the Supporting Information). The two dyes were placed in a diagonally oriented fashion as an energy transfer-based base surrogate pair. This dye arrangement and the sequences of **DNA0–XY** and **RNA0** were derived from our recent siRNA construct with thiazole orange as the energy donor and thiazole red as the energy acceptor, which was used for molecular imaging of siRNA delivery and processing in live cells.[12] To evaluate the best environment for energy transfer between the two dyes, the "counter bases" X and Y were systematically varied (A, G, T, or C). Moreover, the distance between energy donor (dye **1**) and acceptor (dye **2**) was increased from 1 to 3 intervening A–T pairs in **DNA1–DNA3**.

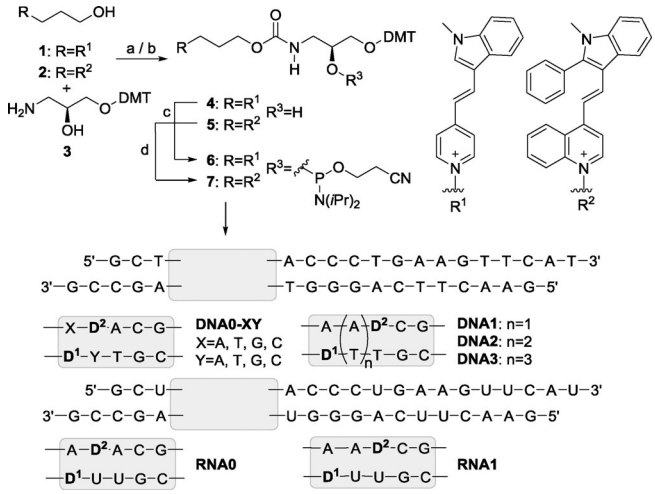

Scheme 2. Synthesis of the building blocks **6** and **7** from dyes **1** and **2**, and sequences of the synthesized oligonucleotides **DNA0–XY**, **DNA1–DNA3**, **RNA0**, and **RNA1** with D^1 (with R^1) and D^2 (with R^2): a) 1,1′-carbonylimidazole, DMF, r.t., 16 h; b) **3**, r.t., 7 d, **4**: 69%, **5**: 56%; c) 2-cyanoethyl *N*,*N*-diisopropylchlorophosphoramidite, CH_2Cl_2, r.t., 16 h, **6**: 99%, **7**: 99%.

The UV/Vis absorption of all doubly modified DNA and RNA duplexes shows the presence of the fluorophores with absorption bands for D^1 at around 470 nm and for D^2 at around 550 nm (see the Supporting Information). The extinction and absorption maxima of both chromophores, D^1 and D^2, as base surrogates show significant differences among the duplexes **DNA0–XY**, and the alterations are more distinct for D^1. This also yields differences in fluorescence readout, as further discussed below. D^1 was selectively excited at 435 nm, and the fluorescence intensities I_{535} and I_{610} at the dye-typical wavelengths 535 nm (D^1) and 610 nm (D^2), respectively, gave information on the energy-transfer efficiency between the two dyes. The best "traffic lights" with respect to the structural variations (counter bases X/Y and distance between D^1 and D^2) were identified by a low fluorescence intensity I_{535} and a high intensity I_{610} and, thereby, a high contrast I_{610}/I_{535} as a characteristic red/green fluorescence readout. Additionally, the enhancement factor f for the red fluorescence was calculated as the major hybridization readout, according to the "traffic light" concept (see Scheme 1). f is the fluorescence ratio I_{610}/I_{535} of the doubly modified double strands (D^1 and D^2) divided by the fluorescence ratio I_{610}/I_{535} of the singly modified single strands (D^1 only). The complete screening of these optical properties (Table 1) revealed that A and T are the best counter bases for both D^1 and D^2; in particular, **DNA0–TA**, **DNA0–TT**, and **DNA0–AT** show emission color contrasts of $I_{610}/I_{535} = 12–34$ and enhancement factors of $f = 72–212$ as fluorescence readouts. It also became obvious that C and G are not suitable as counter bases, neither as X nor as Y. In particular, the fluorescence of the duplexes **DNA0–XC** all show low intensities for the acceptor.

As already described previously,[10] ground-state interactions between two dyes interfere with the energy-transfer process between them. In particular, excitonically coupled dimers of both dyes do not yield an efficient energy transfer, because this requires the selective excitation of the uncoupled energy donor (D^1) in the neighborhood of the uncoupled and, thus, unexcited acceptor (D^2). The absorption maxima λ_{max} of D^1 and D^2 and their ratios A_{maxD1}/A_{maxD2} give more detailed information on this issue. If the distance $\Delta\lambda$ between the two absorption maxima exceeds 84 nm, fluorescence quenching of D^1 is observed, but no efficient energy transfer to D^2. In these cases, the overlap of the D^1 emission and the D^2 absorption, which is crucial for an efficient energy transfer, is low. For instance, this scenario is obvious for **DNA0–AC** with $\Delta\lambda = 102$ nm and $I_{610}/I_{535} = 2.4$. Absorption ratios A_{maxD1}/A_{maxD2} higher than 1.1 indicate excitonic interactions between the dyes that result in higher extinction coefficients for D^1 and lower ones for D^2. These effects are most pronounced in the duplex **DNA0–GG**. The absorption ratio is $A_{maxD1}/A_{maxD2} = 1.61$ and the emission shows almost no energy transfer and mainly quenching. The fluorescence readouts are $I_{610}/I_{535} = 1.1$ and $f = 4.0$, which are the lowest values in these DNA series. This interpretation of ground-state interactions between the dyes was representatively supported by additional optical spectroscopic experiments with **DNA0–GG** (see theSupporting Information). With an excess of the D^2-containing single strand (1.2 equiv), the

Table 1. Summary of optical properties, quantum yields (Φ_F), and melting temperatures (T_m) of the synthesized oligonucleotides.[a]

DNA or RNA	λ_{max} **D**^{1} [nm]	λ_{max} **D**^{2} [nm]	$\Delta\lambda$[b] [nm]	ΔA_{max}[c]	ΔA_{maxss}[d]	$\Delta A_{max}/\Delta A_{ss}$	I_{535}	I_{610}	I_{610}/I_{535}	f	Φ_F **D**^{1}[e]	Φ_F **D**^{2}[f]	T_m [°C]
DNA0–AA	487	551	64	0.78	0.28	2.79	0.25	1.81	7.2	43	0.002	0.182	70
DNA0–TA	492	552	60	0.76	0.32	2.38	0.12	1.52	12.3	72	0.002	0.188	73
DNA0–GA	485	549	64	0.80	0.36	2.67	0.41	1.71	4.1	24	0.014	0.216	68
DNA0–CA	461	546	85	0.71	0.30	2.37	0.19	1.00	5.2	30	0.002	0.094	67
DNA0–AT	487	554	67	0.92	0.45	2.04	0.10	3.55	33.9	212	0.001	0.346	74
DNA0–TT	461	544	83	1.09	0.52	2.10	0.16	2.17	13.0	81	0.002	0.182	71
DNA0–GT	472	555	83	1.34	0.58	2.31	0.89	1.81	2.0	13	0.019	0.124	68
DNA0–CT	458	544	86	1.33	0.49	2.71	0.17	1.08	6.5	40	0.002	0.063	75
DNA0–AC	450	552	102	0.88	0.47	1.87	0.44	1.06	2.4	16	0.003	0.062	70
DNA0–TC	462	546	94	0.86	0.55	1.56	0.28	0.90	3.3	22	0.003	0.056	74
DNA0–GC	486	558	72	1.12	0.61	1.84	0.54	1.31	2.4	16	0.009	0.109	75
DNA0–CC	457	542	85	1.40	0.51	2.75	0.24	0.75	3.1	21	0.009	0.086	73
DNA0–AG	483	556	73	1.32	0.81	1.63	0.23	2.08	8.9	33	0.007	0.229	70
DNA0–TG	473	558	85	1.06	0.94	1.13	0.43	1.84	4.2	16	0.011	0.174	71
DNA0–GG	485	561	76	1.61	1.04	1.55	1.42	1.51	1.1	4	0.076	0.177	73
DNA0–CG	488	558	70	1.16	0.88	1.32	0.62	1.06	1.7	6	0.030	0.128	82
DNA1	478	557	79	0.92	0.44	2.10	0.84	2.65	3.2	20	0.018	0.188	67
DNA2	479	552	73	1.15	0.53	2.17	0.74	3.25	4.4	27	0.027	0.234	67
DNA3	472	549	77	1.19	0.70	1.70	2.11	3.94	1.9	12	0.059	0.241	62
RNA0	481	551	70	1.05	0.58	1.84	0.18	3.59	19.8	99	0.002	0.245	82
RNA1	472	551	79	1.16	0.81	1.43	0.98	4.06	4.1	21	0.019	0.222	80

[a] Conditions: 2.5 μM duplex in 10 mM NaPi buffer,250 mM NaCl, pH 7, 20 °C. [b] $\Delta\lambda = \lambda_{maxD^1} - \lambda_{maxD^2}$. [c] $\Delta A_{max} = A_{maxD^1}/A_{maxD^2}$. [d] $\Delta A_{maxss} = A_{max,ssD^1}/A_{max,ssD^2}$. [e] Excitation 435 nm; emission 450–550 nm. [f] Excitation 435 nm; emission 550–800 nm.

green fluorescence of **D**^{1} is significantly reduced, whereas the red fluorescence of **D**^{2} is not enhanced, but also reduced. Accordingly, it is clearly not the lack of the **D**^{1}-containing strand that limits the energy transfer in **DNA0–GG**. The absorption and excitation spectra further support the ground-state interpretation. With an excess of the **D**^{2}-containing strand, the extinction of **D**^{1} is reduced (although the amount of **D**^{2}-containing strand is higher!), which can be similarly observed in the excitation spectra. Interestingly, all duplexes of the series **DNA0–XG** show the influence of the base environment by a significant red shift of both the absorption and the emission (ca. 5 nm) of **D**^{2}, indicating stacking interactions with G as counter base Y.

The determination of the melting temperatures (T_m) revealed that the duplexes **DNA0–XY** with XY = AT, TA, CG, and GC are higher than the others, which may indicate base pairing of the two "counter bases", thereby controlling the optical properties of the two dyes. The extinction of **D**^{1} in the singly modified single strands is significantly lower than in the corresponding doubly modified duplexes. The absorption ratio A_{maxD1}/A_{maxD2} of the two dyes in two complementary singly modified single strands that were subsequently annealed to the duplex additionally helped to elucidate the best choice of the counter bases X and Y for these dyes. Here, the best "traffic lights" were identified by the A_{maxD1}/A_{maxD2} ratio of the double strand if it was twofold higher than the corresponding ratio in the separated single strands. These observations are particularly valid for **DNA0–AT** with a ratio of 2.04. This apparently optimal duplex with the best optical properties shows an excellent fluorescence readout with $I_{610}/I_{535} = 34$. Together with $f = 212$ and the highest fluorescence intensity of all duplexes, especially an acceptor quantum yield of Φ_F(**D**^{2}) = 35 %, it best fits the requirements for our "traffic lights" and shows a high potential for successful in vivo imaging experiments.

If the interpretation that excitonically coupled fluorophores interfere with energy transfer, it looked reasonable to separate **D**^{1} and **D**^{2} by additional base pairs. This was realized in **DNA1–DNA3** by using the best counter base combination XY = AT (Figure 1). Interestingly, both critical readouts were diminished in these duplexes; the I_{610}/I_{535} ratio dropped from 34 for **DNA0–AT** over 3.1 for **DNA1**, 4.4 for **DNA2** to only 1.9 for **DNA3**, f dropped from 212 to 12. Over such short distances, the relative orientation of the two dyes may control the energy transfer, as studied by Wilhelmsson et al.[19] and Asanuma et al.[20] Clearly, **DNA0–AT** already contains the best possible arrangement and least excitonically coupled fluorophore pair and, thus, shows the best fluorescence readout. With the knowledge on the best energy-transfer arrangement of **D**^{1} and **D**^{2} as base surrogates in DNA double strands, **RNA0** and **RNA1** were prepared with sequences in analogy to **DNA0–AT** and **DNA1**. The fluorescent readout values of these two RNA duplexes were lower compared to their DNA counterparts, owing to the different A-type conformation of double-helical RNA. But, in particular, **RNA0** showed excellent fluorescent readout values with $I_{610}/I_{535} = 20$ and $f = 99$ that make this RNA duplex a promising candidate for in vivo fluorescent imaging.

Representative cell experiments were performed to demonstrate the imaging potential of duplex **DNA0–AT** in living cells. 3×10^4 HeLa cells were transfected with 15 pmol of **DNA0–AT** and ScreenFect®A for 24 h and imaged by confocal fluorescent microscopy using an excitation wavelength of 488 nm (Figure 2). To demonstrate the energy transfer, the emission of the energy donor **D**^{1} (λ_{em} = 490–530 nm) and the emission of the energy acceptor **D**^{2} (λ_{em} = 650–790 nm) were separately de-

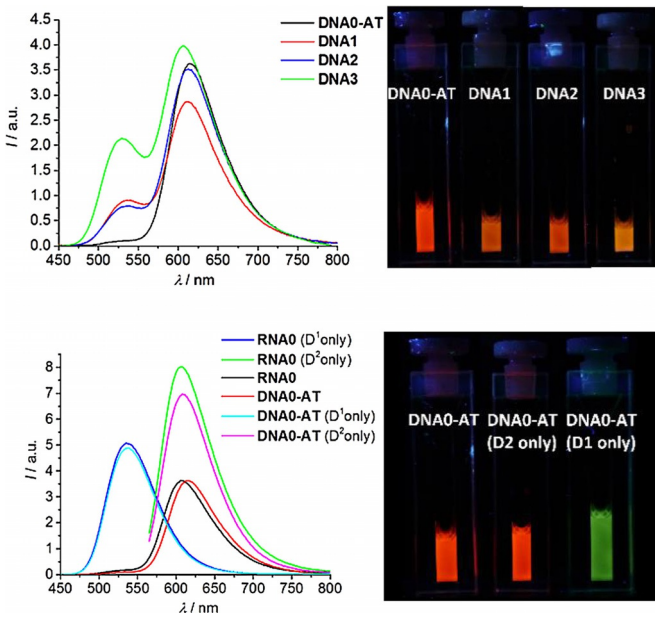

Figure 1. Fluorescence of **DNA0–AT**, **DNA1–DNA3** to elucidate the distance dependency for the optimal counter base combination AT (top); fluorescence of **DNA0–AT** and **RNA0** in comparison with the corresponding reference double strands that were modified only by single dyes ("D^1only" or "D^2only") (bottom): 2.5 μM double strand, 10 mM Na-P_i buffer, 250 mM NaCl, pH 7, 25 °C, λ_{exc} = 435 for energy transfer, λ_{exc} = 550 nm for "$\mathbf{D^2}$ only". The images illustrate the fluorescence using a handheld UV lamp.

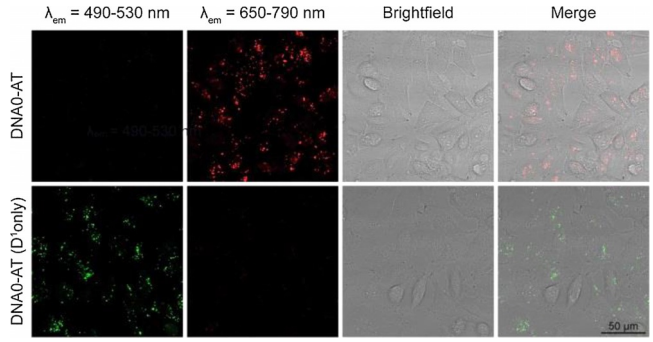

Figure 2. Confocal images of HeLa cells after transfection with the doubly modified **DNA0–AT** (top) and the corresponding reference duplex that was modified only with $\mathbf{D^2}$ (bottom). The visualization was performed by using a laser scanning confocal fluorescence microscope Leica TCS -SP8 equipped with a Leica DMI8-CS inverted microscope and a HCPL APO CS2 40x/1.10 WATER objective. The cells were exited with an argon laser (λ_{exc} = 488 nm) and the emission was detected at λ_{em} = 490–530 nm and 650–790 nm; scale bar 50 μm.

tected. The images revealed that the transfection of the doubly modified DNA was successful and that the FRET occurred nearly quantitatively, which is shown by the fluorescence at λ_{em} = 650–790 nm. Control experiments with a reference duplex modified with $\mathbf{D^2}$ exclusively showed fluorescence at λ_{em} = 490–530 nm. It became clear that the energy transfer between the two base surrogates $\mathbf{D^1}$ and $\mathbf{D^2}$ worked as an efficient energy-transfer pair in living cells and in vitro.

3. Conclusions

Two new DNA/RNA building blocks were synthesized, which carry the cyanine–styryl dyes **1** and **2** that were previously evaluated as very photostable alternatives to thiazole orange and thiazoel red, and (*S*)-3-amino-1,2-propanediol as a substitute for the ribofuranoside. By using these building blocks, both dyes were successfully incorporated into DNA and RNA through automated solid-phase chemistry. Excitation of the green-emitting $\mathbf{D^1}$ in the double strand led to an energy transfer to $\mathbf{D^2}$ and yielded red light emission, whereas the single strand showed only green fluorescence. This fluorescent readout was characterized by the red/green emission color contrast I_{610}/I_{535} and the fluorescence enhancement factor *f*. The screening comprised of duplexes, in which the counter bases X and Y to $\mathbf{D^1}$ and $\mathbf{D^2}$, respectively, were varied and the distance between the dyes was enlarged from 0 to 3 intervening AT base pairs. The best readout was obtained for the combination with X = A as counter base to $\mathbf{D^1}$ and Y = T as counter base to $\mathbf{D^2}$. Separating the dyes as a base surrogate pair by additional A–T base pairs did not improve the readout. In particular, **DNA0–AT** showed excellent fluorescence readout with I_{610}/I_{535} = 34, *f* = 212, and an acceptor quantum yield of $\Phi_F(\mathbf{D^2})$ = 35 %. This duplex did not only suit the requirements of our "traffic light" concept for in vivo imaging experiments, but also showed significantly better fluorescence properties compared to our previous DNA and RNA "traffic lights" based on thiazole orange and thiazole red as the base surrogate pair. In comparison to our recently published post-synthetic modification of the 2′-position of uridine (in the ribo and arabino configuration),[21] the quantum yields of the base surrogate approach (as presented herein) were significantly higher. An additional advantage in comparison to the post-synthetically modified DNA and RNA samples was the avoidance of copper (I) that may interfere with cellular experiments, owing to its cytotoxicity. This offered the application for in vivo imaging experiments, which was representatively demonstrated for **DNA0–AT**. Fluorescence confocal microscopy revealed that the energy transfer could also be obtained in living cells. In summary, the two cyanine–styryl dyes **1** and **2** as base pair surrogates in DNA as well as in RNA efficiently form an energy-transfer pair, giving rise to a very promising tool for molecular imaging.

Experimental Section

All experimental details are described in the Supporting Information.

Acknowledgements

Financial support by the Deutsche Forschungsgemeinschaft (GRK 2039), the Helmholtz program "Biointerfaces in Technology and Medicine (BIFTM)", and KIT is gratefully acknowledged.

Conflict of Interest

The authors declare no conflict of interest.

Keywords: chromophores · energy transfer · fluorescence · imaging · oligonucleotides

[1] a) Q. Shao, B. Xing, *Chem. Soc. Rev.* **2010**, *39*, 2835 – 2846; b) P. V. Chang, C. R. Bertozzi, *Chem. Commun.* **2012**, *48*, 8864 – 8879; c) Q. Zheng, M. F. Juette, S. Jockusch, M. R. Wasserman, Z. Zhou, R. B. Altman, S. C. Blanchard, *Chem. Soc. Rev.* **2014**, *43*, 1044 – 1056; d) K. M. Dean, A. E. Palmer, *Nat. Chem. Biol.* **2014**, *10*, 512 – 523.

[2] a) B. B. A. Armitage, *Curr. Opin. Chem. Biol.* **2011**, *15*, 806 – 812; b) U. Rieder, N. W. Luedtke, *Angew. Chem. Int. Ed.* **2014**, *53*, 9168 – 9172; *Angew. Chem.* **2014**, *126*, 9322 – 9326; c) F. Hövelmann, O. Seitz, *Acc. Chem. Res.* **2016**, *49*, 714 – 723; d) Z. Li, T. M. Rana, *Acc. Chem. Res.* **2012**, *45*, 1122 – 1131; e) J. Nguyen, F. C. Szoka, *Acc. Chem. Res.* **2012**, *45*, 1153 – 1162; f) K. Raemdonck, K. Remaut, B. Lucas, N. N. Sanders, J. Demeester, S. C. De Smedt, *Biochemistry* **2006**, *45*, 10614 – 10623; g) K. A. Whitehead, R. Langer, D. G. Anderson, *Nat. Rev. Drug Discovery Nat. Rev. Drug Discov.* **2009**, *8*, 129 – 138.

[3] a) W. Schmucker, H.-A. Wagenknecht, *Synlett* **2012**, *23*, 2435 – 2448; b) M. Merkel, K. Peewasan, S. Arndt, D. Ploschik, H.-A. Wagenknecht, *ChemBioChem* **2015**, *16*, 1541 – 1553.

[4] S. H. Weisbrod, A. Marx, *Chem. Commun.* **2008**, 5675 – 5685.

[5] a) H. Asanuma, M. Akahane, N. Kondo, T. Osawa, *Chem. Sci.* **2012**, *3*, 3165 – 3169; b) H. Kashida, T. Osawa, K. Morimoto, Y. Kamiya, H. Asanuma, *Bioorg. Med. Chem.* **2015**, *23*, 1758 – 1762.

[6] F. Hövelmann, L. Bethge, O. Seitz, *ChemBioChem* **2012**, *13*, 2072 – 2081.

[7] N. Amann, R. Huber, H.-A. Wagenknecht, *Angew. Chem. Int. Ed.* **2004**, *43*, 1845 – 1847; *Angew. Chem.* **2004**, *116*, 1881 – 1883.

[8] T. Ehrenschwender, H.-A. Wagenknecht, *J. Org. Chem.* **2011**, *76*, 2301 – 2304.

[9] C. Holzhauser, S. Berndl, F. Menacher, M. Breunig, A. Göpferich, H.-A. Wagenknechr, *Eur. J. Org. Chem.* **2010**, 1239 – 1248.

[10] S. Barrois, S. Wörner, H.-A. Wagenknecht, *Photochem. Photobiol. Sci.* **2014**, *13*, 1126 – 1129.

[11] C. Holzhauser, H.-A. Wagenknecht, *J. Org. Chem.* **2013**, *78*, 7373 – 7379.

[12] C. Holzhauser, R. Liebl, A. Göpferich, H.-A. Wagenknecht, M. Breunig, *ACS Chem. Biol.* **2013**, *8*, 890 – 894.

[13] M. Rubner, C. Holzhauser, P. Bohländer, H.-A. Wagenknecht, *Chem. Eur. J.* **2012**, *18*, 1299 – 1302.

[14] P. R. Bohländer, H.-A. Wagenknecht, *Meth. Appl. Fluoresc.* **2015**, *3*, 044003.

[15] P. Bohländer, H.-A. Wagenknecht, *Org. Biomol. Chem.* **2013**, *11*, 7458 – 7462.

[16] H.-K. Walter, P. R. Bohländer, H.-A. Wagenknecht, *ChemistryOpen* **2015**, *4*, 92 – 96.

[17] R. Huber, N. Amann, H.-A. Wagenknecht, *J. Org. Chem.* **2004**, *69*, 744 – 751.

[18] J. C. Schulhof, D. Molko, R. Teoule, *Nucl. Acids Res.* **1987**, *15*, 397 – 416.

[19] K. Börjesson, S. Preus, A. H. El-Sagheer, T. Brown, B. Albinsson, L. M. Wilhelmsson, *J. Am. Chem. Soc.* **2009**, *131*, 4288 – 4293.

[20] T. Kato, H. Kashida, J. Kishida, H. Yada, H. Okamoto, H. Asanuma, *J. Am. Chem. Soc.* **2013**, *135*, 741 – 750.

[21] H.-K. Walter, B. Olshausen, U. Schepers, H.-A. Wagenknecht, *Beilstein J. Org. Chem.* **2017**, *13*, 127 – 137.

Received: March 22, 2017
Version of record online June 7, 2017

